RZ 3870 (#ZUR1403-036) 03/19/2014
Physical Sciences 6 pages

Research Report

Image correction for atomic force microscopy images with functionalized tips

M. Neu,[1] N. Moll,[2] L. Gross,[2] G. Meyer,[2] F. J. Giessibl,[1] and J. Repp[1]

[1]Institute of Experimental and Applied Physics, University of Regensburg, 93053, Germany

[2]IBM Research – Zurich, 8803 Rüschlikon, Switzerland

The final version of this paper appeared in *Phys. Rev. B* **89**, 205407 (7 May 2014) and may be downloaded at http://dx.doi.org/10.1103/PhysRevB.89.205407

Image correction for atomic force microscopy images with functionalized tips

M. Neu,[1] N. Moll,[2] L. Gross,[2] G. Meyer,[2] F. J. Giessibl,[1] and J. Repp[1]

[1] *Institute of Experimental and Applied Physics, University of Regensburg, 93053, Germany*
[2] *IBM Research–Zurich, 8803 Rüschlikon, Switzerland*

(Dated: February 23, 2014)

It has been demonstrated that atomic force microscopy imaging with CO-functionalized tips provides unprecedented resolution, yet it is subject to strong image distortions. Here we propose a method to correct for these distortions. The lateral force acting on the cantilever is calculated from three-dimensional maps of the frequency shift signal. Assuming a linear relationship between lateral distortion and force, atomic force microscopy images could be deskewed for different substrate systems.

PACS numbers: 68.37.-d,68.37.Ps,68.43.Fg

I. INTRODUCTION

The possibility to reveal the chemical structure of individual molecules by means of AFM has recently been enabled by using functionalized tips[1]. Whereas different tip functionalizations have been reported[2,3], CO was used most often, now being widely applied[2–14]. Unfortunately, the molecular geometry appears considerably distorted in these images – an effect that is attributed to the bending of the CO-molecule at the tip apex because of its interaction with the sample[15]. This effect leads to an apparent sharpening of bonds[15] and increases the lateral size of features arising from individual atoms[9,16]. Whereas in many cases a slight distortion of the images may not compromise the experimental findings, in some cases the detailed geometric structure itself bares crucial information[17]. As the positions of atoms appear displaced by distances on the order of 1 Å, this effect may also prevent a site determination of adsorbates of low symmetry.

Here, we present a technique to correct for the image distortions that are due to this effect. The correction is based on the assumption that the bending of the CO molecule at the tip apex is in good approximation linear to the lateral forces acting on the cantilever. The latter can be derived from three-dimensional (3D) maps of the frequency shift Δf of the force sensor by subsequent integration and differentiation[18–20]. As the scaling constant of the distortion with lateral force is unknown, it needs to be extracted from a known structure, which can be a functional group of known geometry of the molecule under study. Here, we successfully apply the proposed method to deskew images of pentacene molecules adsorbed on bare copper and on NaCl films, respectively.

II. METHODS

Experiments are performed using a homebuilt qPlus-based[21] AFM in ultra high vacuum ($p \approx 5 \cdot 10^{-11}$ mbar) at low temperatures of 5 K. Sodium chloride was evaporated onto clean Cu(111) surface at sample temperatures of about 277 K. Pentacene was adsorbed at sample temperatures below 10 K. CO was dosed onto the sample for tip functionalization. The sensor is characterized by its resonance frequency of $f_0 = 26.057$ kHz, its stiffness of $k = 1800$ N/m, and its quality factor of $Q \approx 13\,000$. The AFM was operated in the frequency modulation mode (FM-AFM[22,23]) while keeping the oscillation amplitude constant at 0.45 Å. The images were acquired in the constant height mode at zero sample voltage for different tip-sample distances.[24]

To minimize creep, the tip was held in constant current mode for more than 12 h at STM set-point parameters of 1 pA and 400 mV before the entire set of constant-height $\Delta f(x, y)$ images at given tip-height values was acquired. Between the acquisition of each two subsequent images, the feedback-loop was switched on for several seconds. During the entire data acquisition no tip changes were observed and a cross-correlation analysis of the images revealed that drift was negligible.

III. RESULTS AND DISCUSSION

Figure 1 shows atomically resolved Δf images of pentacene on bare Cu(111) (top panel) as well as on a bilayer of NaCl on Cu(111) (bottom panel), respectively. Superimposed on the experimental images are the positions of the carbon atoms, for the well-known geometry of pentacene[25]. From these, the distortions can be estimated to be of up to roughly 0.6 Å on Cu(111) and 1.4 Å on NaCl/Cu(111), respectively, leading to an apparent increase in the C–C bond lengths of up to approximately 40% and 100%. These apparent elongations are much larger than the experimental uncertainty of the image scaling and the expected bond length changes that could arise from the interaction of pentacene with the substrate. As the distortions are thought to be due to the bending of the CO-molecule at the tip apex[15], it should be possible to correct for the distortions, if the forces acting on the CO can be experimentally determined. To correct for the image distortion in the simplest possible way, we assume the in-plane distortion (that is, parallel to the surface) $\Delta\vec{r}_{\parallel}$ to scale linear with the corresponding

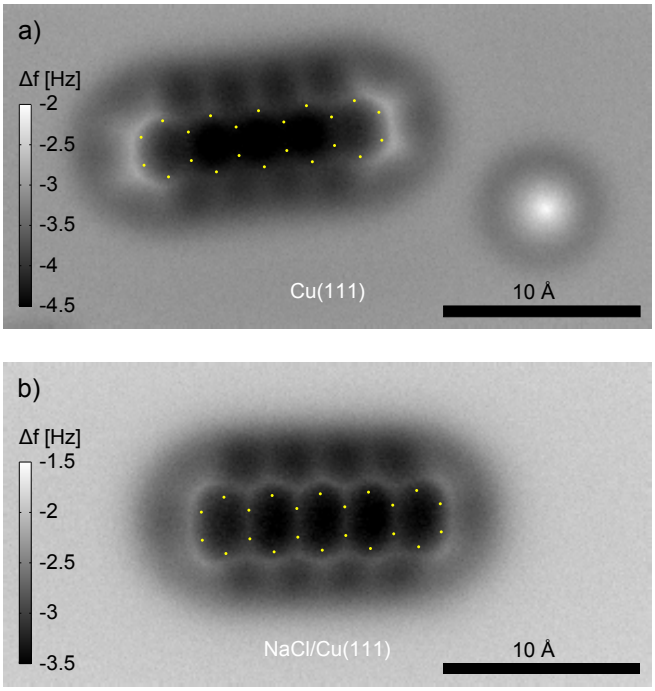

FIG. 1. Pentacene adsorbed on a) bare Cu(111) and b) NaCl/Cu(111) was imaged by recording the frequency shift Δf at a constant height of $z' = 0$. Dots indicate the positions of carbon atoms in the known geometry of pentacene. In comparison, one realizes that the molecule's geometric structure appears distorted. This effect is attributed to a bending of the CO due to forces acting on it. The distortions are considerably larger on the NaCl substrate as compared to the case of adsorption on the bare copper. In the right part of the image in the top panel there is a CO molecule on the surface.

forces $\vec{F}_\parallel$ with a certain unknown scaling constant α as

$$\Delta\vec{r}_\parallel = \alpha\vec{F}_\parallel. \tag{1}$$

The scaling constant α has the dimension of the inverse of a spring constant. Even though related, it is not simply the inverse of the stiffness of the CO molecule at the tip apex as will be discussed further below. In FM-AFM the tip-sample interaction results in a frequency shift Δf[26]. Using small oscillation amplitudes of the cantilever, the frequency shift Δf with respect to the eigenfrequency without tip-sample interaction f_0 is in good approximation proportional to the vertical force gradient

$$\frac{\partial F_\perp}{\partial z} \approx -\frac{2\cdot k}{f_0}\cdot\Delta f \tag{2}$$

where $F_\perp$ is the out-of-plane component of the force and k is the stiffness of the cantilever[27]. Integrating $\partial F_\perp/\partial z$ twice along z yields the tip-sample interaction potential, the lateral gradient of which provides the lateral tip-sample forces[19]

$$\vec{F}_\parallel = -\frac{2\cdot k_0}{f_0}\cdot\vec{\nabla}_\parallel\left(\iint\Delta f\,\mathrm{d}^2z\right). \tag{3}$$

Hence, a 3D map of $\Delta f(x,y,z)$ is needed in order to extract the lateral forces and to correct the distortions in the images. There are two conceptually different ways to obtain 3D-Δf-maps, namely, one may acquire many $\Delta f(z)$ spectra on a two-dimensional grid of (x,y)-values[18,28], or many constant-height $\Delta f(x,y)$ images at a given set of z-values[20] above the molecule. While both methods have their own advantages, we here make use of the latter, as it allows for a high spatial resolution at a reasonable data-acquisition time.

$\Delta f(x,y,z)$ changes much more rapidly with z for short tip-sample distances than for large ones. We therefore chose the set of z-values, at which we acquired Δf maps, to be non-equidistant with the sampling becoming more dense with decreasing tip-sample separations. For each 3D map we acquired 40 images. The intra-molecular resolution was shown to be due to Pauli repulsion between tip and molecule[15], which is very short-range in nature and should therefore depend sensitively on the actual tip-molecule separation. In contrast, attractive interactions are expected to laterally vary only slowly over the molecule. Therefore, we expect that the appearance of intra-molecular resolution occurs at a comparable tip-molecule separation for adsorption on different substrates (when determined with the same tip apex under identical imaging conditions).

To this end, we determined the tip height at which intra-molecular resolution on pentacene starts to appear. From this height, the tip was moved by 0.85 Å closer to the sample to acquire the atomically resolved images, shown in Fig. 1. These images are the ones that are to be deskewed, and we defined the tip-sample distance at which they were acquired as $z' = 0$. The local minima of $\Delta f(z')$ spectra may also be used as a reference for the tip-adsorbate distance[14,17]. Here, these minima occur at $z' \simeq 0.2$ Å for spectra acquired at the center of one of the two outermost carbon rings on both substrates[29], supporting that $z' = 0$ corresponds indeed to the same tip-adsorbate distance on both substrates.

According to eq. 3, Δf-data is numerically integrated twice along the z-axis and then differentiated laterally to obtain the in-plane component of the force $\vec{F}_\parallel$. Here, we reverse the sequence of integration and differentiation as

$$\vec{F}_\parallel = -\frac{2\cdot k_0}{f_0}\cdot\iint\left(\vec{\nabla}_\parallel\Delta f\right)\mathrm{d}^2z. \tag{4}$$

This has the advantage that the quantity $\vec{\nabla}_\parallel\Delta f$ can be analyzed separately for each image, providing an understanding of its influence on the total lateral forces as discussed further below. In the experiment, one has a discrete set of Δf maps at n different tip sample distances z_i. If those are equidistant in z, at a spacing of δz, eq. 4 becomes

$$\vec{F}_\parallel = -\frac{2\cdot k_0\cdot\delta z^2}{f_0}\cdot\sum_{i=1}^{n}(n-i+1)\left(\vec{\nabla}_\parallel\Delta f(x,y,z_i)\right). \tag{5}$$

Note that the integration, and hence the summation, has to proceed from large to short tip-molecule distances.

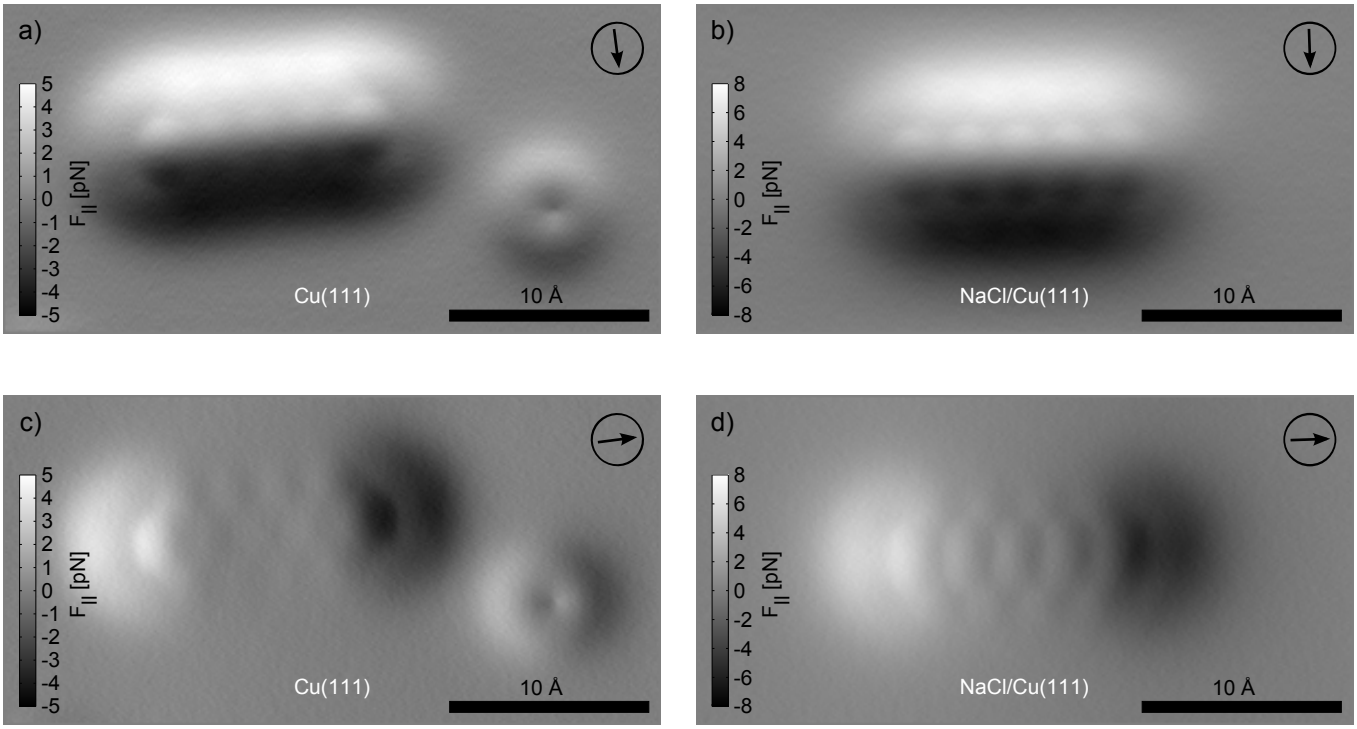

FIG. 2. Component of the lateral force between tip and sample above an individual pentacene molecule along the high-symmetry directions of the molecule at $z' = 0$.The lateral force of pentacene (and CO) on clean Cu(111) (a and c) and pentacene on NaCl (b and d) are shown with respect to the short and long axis of the molecule (directions as indicated by the arrows). The main contribution is a force pointing towards the center of the molecule. In order to reflect mainly the lateral forces acting on the CO molecule of the functionized tip, the integration of Δf has been limited to $z' = 3.95$Å. On the NaCl substrate, the lateral force is considerably larger compared to the Cu substrate.

Hence, $\delta z(n - i + 1) = z_i - z_F$, where z_F is the position of the final image that is to be deskewed and where the forces need to be determined. Thus,

$$\vec{F}_{\parallel} = -\frac{2 \cdot k_0 \cdot \delta z}{f_0} \cdot \sum_{i=1}^{n} (z_i - z_F) \left(\vec{\nabla}_{\parallel} \Delta f(x, y, z_i) \right). \quad (6)$$

An analogous derivation for a non-equal z-spacing of Δf yields

$$\vec{F}_{\parallel} = -\frac{2 \cdot k_0}{f_0} \cdot \sum_{i=1}^{n} \delta z_i \cdot (z_i - z_F) \left(\vec{\nabla}_{\parallel} \Delta f(x, y, z_i) \right), \quad (7)$$

where δz_i is the z-spacing at the Δf-image i. Note that the factor $(z_i - z_F)$ weights the contributions in $\Delta f(x, y)$-images increasingly for increasing z_i. Here, z' was defined such that z_F corresponds to $z' = 0$, and $z_i - z_F = z'_i$.

Fig. 2 shows the calculated lateral forces above pentacene adsorbed on Cu and on NaCl, respectively, at $z' = 0$. To obtain these, the integration (i. e., the summation in eq. 7) was performed of up to $z' = 3.95$ Å. Obviously, the lateral forces in the case of pentacene on NaCl are substantially larger than on copper. The same holds true for the distortions in the AFM images (cf. Fig. 1).

To obtain the lateral forces acting on the entire tip, the integration has to be performed up to z-values, at which $\Delta f(x, y)$ does no longer vary laterally. However, only the forces that act on the CO molecule give rise to the image distortion, whereas the measured $\Delta f(x, y)$ results from the forces acting on the entire tip. Unfortunately, the ratio between the forces acting on the metal tip and the CO molecule depends on the tip-sample distance: Pauli repulsion occurs only at short distances and will primarily act on the CO molecule. Van-der-Waals attraction is dominating at intermediate distances and will act on both the CO molecule and the metal tip apex[1]. Finally, forces arising from local contact potential differences are dominant at large distances ($z' \gtrsim 3$ Å) and will primarily act on the metal tip apex.

It is therefore crucial to analyze the lateral gradient of the frequency signal $\vec{\nabla}_{\parallel} \Delta f(x, y)$, the integration of which will result in the lateral forces for these different regimes. As has been pointed out above (eq. 7), the influence of contributions in $\Delta f(x, y)$-images increases with distance z. On the other hand, the corrugation in $\Delta f(x, y)$-images fades away with increasing distance from the surface. To understand the influence of $\Delta f(x, y)$-images at different distances to the resulting lateral force, we determined the quantity $(z_i - z_F) \cdot \iint \left| \vec{\nabla}_{\parallel} \Delta f(x, y) \right| \mathrm{d}x \, \mathrm{d}y$. This quantity is displayed for pentacene on Cu(111) in Fig. 3c, and it is a measure of the contribution of a particular $\Delta f(x, y)$-

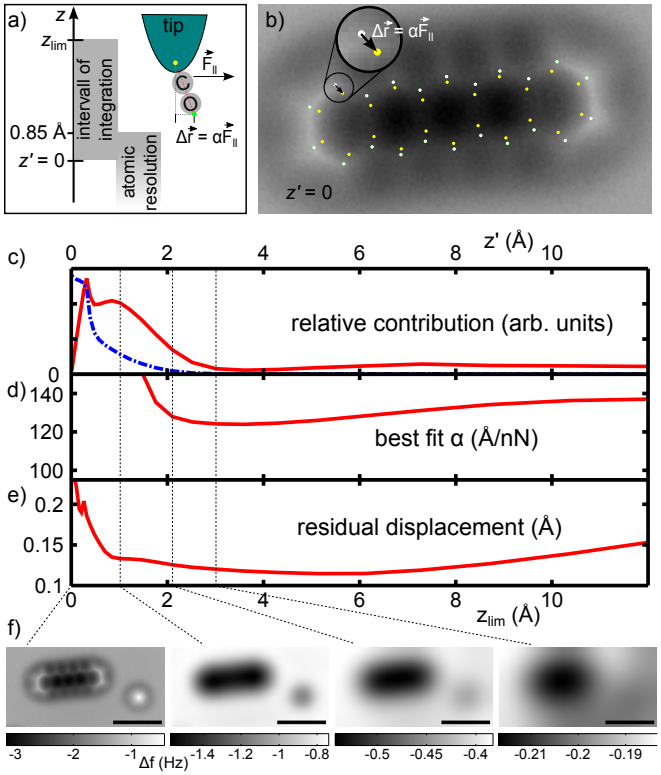

FIG. 3. a) Schematic illustration of the geometry and definition of z' and $z_{\rm lim}$. b) The coordinates of the positions at which one would expect the carbon atoms of pentacene on Cu(111) in the distorted AFM images are indicated in white, their positions according to the known structure of pentacene in yellow. Based on these positions and the experimentally determined forces, the scaling factor α can be determined from linear regression. The dash-dotted line in c) shows the averaged absolute lateral gradient of each image. This is a relative measure of the corrugation in each image. The solid line represents the same quantity multiplied with z' and is a measure of the relative contribution of each image to the resulting lateral force at $z' = 0$. The largest contribution to the lateral forces arises from Δf data in the range of $0.2 \lesssim z' \lesssim 3$Å. The best fit of the scaling constant α is displayed in d) as a function of the upper limit of integration $z_{\rm lim}$ when evaluating the lateral forces. The corresponding residual displacement of carbon atoms in the corrected image is shown in e). A selected sub-set of Δf images in f) shows that the largest contribution to the lateral forces arises from the 'bath-tub' like depression in these images. Scale bars are 10Å.

image to the resulting lateral force.

As reported earlier[1], at intermediate distances (for $z' \lesssim 3$ Å), the pentacene gives rise to a 'bath tub' shaped depression in constant-height $\Delta f(x, y)$ images[1]. This contribution arises from the van-der-Waals attraction and corresponds to forces pointing always towards the center of the molecule. This feature results in the main contribution of the lateral force, and hence the main correction to the lateral size of the molecular shape, see Fig. 3f. For larger distances, the 'bath tub' feature fades more rapidly than the linear increase of its influence onto the lateral forces. Compared to the 'bath tub' shaped depression, the intra-molecular features result only in a smaller contribution to the lateral forces as they emerge only at the last few tenths of Ångstroms. At large distances, the $\Delta f(x, y)$ signal is dominated by electrostatic forces. Even though the $\Delta f(x, y)$ signal at these distances is small, it still results in appreciable lateral forces acting on the cantilever, as can be seen in Fig. 3c. However, as argued above, these will act primarily on the metal part of the tip and do not reflect the forces acting on the CO molecule.

To determine the best fit of the free parameter α and to quantify the goodness of the correction, we determined the coordinates of the positions at which one would expect the carbon atoms of pentacene in the distorted AFM images, as is illustrated in Fig. 3b. On average, these positions differ from the known structure of pentacene by 0.43Å and 0.80Å for pentacene on clean Cu(111) and on NaCl/Cu(111), respectively. Based on the experimentally determined lateral force (cf. equation 7) these positions are shifted according to relation 1 (cf. Fig. 3a). This allows to obtain a best fit of the free parameter α from linear regression. As argued above, the upper limit of the vertical integration (or summation) may influence the result. To quantify this, we determined the lateral force for all possible upper limits $z_{\rm lim}$ and plotted the best fit of α as well as the residual apparent lateral displacement of carbon atoms as a function of $z_{\rm lim}$, as shown in Fig. 3d and e, respectively. In agreement with the above considerations, we observe that for an upper limit of 3-5Å the corrections are best. An integration to even larger distances only reduces the quality of the correction. Interestingly, in this region α barely varies with $z_{\rm lim}$. We therefore chose $z_{\rm lim} = 3.95$ Å for the image correction, as was also done for calculating the lateral forces shown in Fig. 2. This integration range included 17 images for each data set. The image correction reduces the average apparent displacement of carbon atoms in pentacene from 0.43Å in the raw data to only 0.12Å. Note that the latter distance is comparable to the size of an individual pixel in the original images.

To correct the entire image for its distortions, we shift each pixel in the image by $\Delta\vec{r}_{\parallel}$ as explained above (cf. equations 1 and 7) using the best fit of $\alpha = 123$ Å/nN. As can be seen in Fig. 1, the distortions at different positions within one single molecule as well as for the two images on bare Cu(111) and on NaCl/Cu(111), respectively, are quite different. Most importantly, we can correct both images reasonably well with the very same value for the parameter α, as is shown in Fig. 4. This supports the assumption that the distortions and the lateral forces are roughly proportional to each other and corresponds to the observation that on NaCl not only the distortions but also the lateral forces (cf. Fig. 2) are roughly twice as large as compared to adsorption on bare copper. A detailed best fit analysis performed analogously for pentacene on NaCl/Cu(111) yields that also for this case an

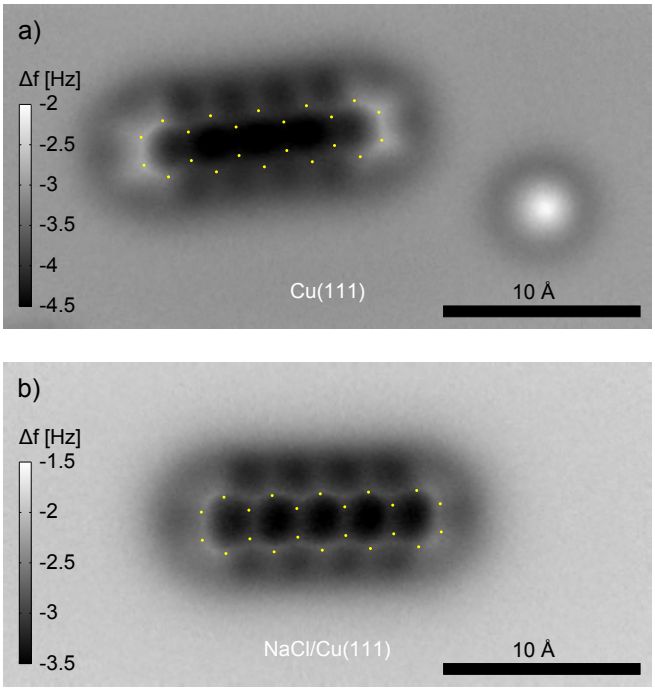

FIG. 4. Deskewed images of individual pentacene molecules at $z' = 0$.The images shown in Fig. 1 are deskewed by means of the lateral force shown in Fig. 2 for Pentacene adsorbed a) on Cu(111) and b) on NaCl/Cu(111).

upper limit z_{lim} of 3-5Å works best. It yields a slightly larger value for α of $\alpha = 140\,$Å/nN, resulting in an average displacement being reduced from an initial value of 0.80Å without image correction to 0.18Å for the corrected case. Hence, in both cases the correction reduces the distortions by approximately a factor of four.

The observation that the integration has to be limited to roughly $z_{\mathrm{lim}} \simeq 4\,$Å greatly reduces the experimental effort for image correction, as only a very limited set of Δf-images has to be recorded as input to the correction algorithm. To investigate this further, we chose a subset of only four of the images from the dataset acquired on pentacene on Cu(111) at distances $z' \simeq 1.0$, 2.1, 3.0 and 4.3 Å, respectively, and we used only these for the image correction. Even with this small number of images, the correction yields good results ($\alpha = 138\,$Å/nN with a residual average displacement of 0.13Å).

Finally, we repeated the above described experiments for a different tip apex, also terminated with a CO molecule. In the image obtained with this apex the atomic structure of pentacene and the 'bath-tub' feature were slightly displaced against each other, indicating a slightly asymmetric tip apex. With an optimal scaling constant of $\alpha = 116\,$Å/nN the average displacement could be reduced from 0.55Å to 0.17Å, in this case.

We assume that there is no universal value for the optimal scaling constant α, so that it has to be separately determined for each individual tip apex. It may well be that the effective lateral stiffness of the CO at the tip apex depends on the details of the individual tip apex. Even more likely, the ratio of the force that acts on the CO and on the rest of the tip will probably vary from tip to tip. However, for a given tip, α can be extracted from a known structure, which can be a part of the molecule under study. We note that when imaging at even closer tip-sample distance, we do not expect this method to still produce reasonable corrections, since in this regime the linear scaling in eq. 1 will be justified no longer.

The bending of the CO changes along the vertical integration path from large to small tip-sample separations. One may account for this bending by correcting each individual image along the integration path and hence integrate over corrected images. We tested this type of correction against the simpler case of integration of the uncorrected data, where only the final image is corrected. Whereas there are no appreciable differences for both methods, the first is more susceptible to noise, as there the noise will also affect the integration pathway. As is discussed above, the main contribution to the lateral forces result from the images in the range of $0.2 \lesssim z' \lesssim 3$Å, in which the contrast varies only on the Ångstrom but not on the sub-Ångstrom scale. Bearing this in mind, it is not surprising that the correction as proposed above does not result in a significant improvement over the simpler correction method.

As pointed out above, α does not directly correspond to the inverse of the stiffness of the CO molecule attached to the tip. The stiffness of the CO is not only determined by its bonding to the tip apex but also by its attractive interaction with the substrate. The vertical force resulting from the latter was previously determined to be up to 80 pN[1] for similar imaging conditions. If we use the same moment arm as Weymouth *et al.* of 3.02 Å[30], this vertical force alone results in a stiffness of the CO molecule of 0.26 N/m, even if there are no other restoring forces. This stiffness is a factor of three larger than the value of $1/\alpha$, underscoring that the two quantities are not at all the same. A difference in these two quantities arises firstly because the experimentally determined force $\vec{F}_{\|}$ reflects not only forces acting on the CO molecule but also those acting on the metal tip apex. Secondly, the lever arm of AFM imaging will be different from the moment arm of $\vec{F}_{\|}$. Thirdly, the cut-off of the integration at a limit of z' neglects some unkown fraction of $\vec{F}_{\|}$. However, even under consideration of the above, the discrepancy of a factor of three is still surprisingly large.

As previously pointed out, the intra-molecular contrast in AFM images on molecules with a CO-functionalized tip arises from Pauli-repulsion, which results from the electron density overlap between tip and sample. Hence, the lateral positions of largest repulsion in a constant-height AFM image correlate with the maxima in charge density of the sample at a given height[15], which are not necessarily located exactly above the atomic nuclei. This effect—going beyond the scope of this work—will also change the apparent positions of atoms in the AFM images in addition to the bending of the CO molecule at

the tip apex. It can be accounted for by computing the positions of highest electron density above the molecule and, instead of the molecular geometry, comparing these with the AFM images.

IV. CONCLUSION

We have proposed a technique to deskew experimental AFM images that have been obtained with functionalized tips. The correction is based on the assumption that the distortions depend linearly on the lateral forces, which can be determined experimentally. Such a correction reduces the image distortions by approximately a factor of four. Distortions in AFM images of pentacene on Cu and on NaCl can be corrected with similar scaling constants, despite the distortions of the original images in both cases being quite different.

ACKNOWLEDGMENTS

We thank Gerhard Münnich and Jay Weymouth for fruitful discussions. Financial support from the Volkswagen Foundation (Lichtenberg program), the Deutsche Forschungsgemeinschaft (SPP 1243), and the ERC Advanced Grant CEMAS is gratefully acknowledged.

[1] L. Gross, F. Mohn, N. Moll, P. Liljeroth, and G. Meyer, Science **325**, 1110 (2009).
[2] F. Mohn, B. Schuler, L. Gross, and G. Meyer, Appl. Phys. Lett. **102**, 073109 (2013).
[3] G. Kichin, C. Wagner, F. S. Tautz, and R. Temirov, Phys. Rev. B **87**, 081408 (2013).
[4] L. Gross, F. Mohn, N. Moll, G. Meyer, R. Ebel, W. M. Abdel-Mageed, and M. Jaspars, Nature Chemistry **2**, 821 (2010).
[5] L. Gross, N. Moll, F. Mohn, A. Curioni, G. Meyer, F. Hanke, and M. Persson, Phys. Rev. Lett. **107**, 086101 (2011).
[6] Z. Sun, M. P. Boneschanscher, I. Swart, D. Vanmaekelbergh, and P. Liljeroth, Phys. Rev. Lett. **106**, 046104 (2011).
[7] N. Pavliček, B. Fleury, M. Neu, J. Niedenführ, C. Herranz-Lancho, M. Ruben, and J. Repp, Phys. Rev. Lett. **108**, 086101 (2012).
[8] M. P. Boneschanscher, J. van der Lit, Z. Sun, I. Swart, P. Liljeroth, and D. Vanmaekelbergh, ACS Nano **6**, 10216 (2012).
[9] J. Welker and F. J. Giessibl, Science **336**, 444 (2012).
[10] F. Albrecht, M. Neu, C. Quest, I. Swart, and J. Repp, J. Am. Chem. Soc. **135**, 9200 (2013).
[11] D. G. de Oteyza, P. Gorman, Y.-C. Chen, S. Wickenburg, A. Riss, D. J. Mowbray, G. Etkin, Z. Pedramrazi, H.-Z. Tsai, A. Rubio, M. F. Crommie, and F. R. Fischer, Science **340**, 1434 (2013).
[12] J. van der Lit, M. P. Boneschanscher, D. Vanmaekelbergh, M. Ijs, A. Uppstu, M. Ervasti, A. Harju, P. Liljeroth, and I. Swart, Nature Communications **4**, 2023 (2013).
[13] J. Zhang, P. Chen, B. Yuan, W. Ji, Z. Cheng, and X. Qiu, Science **342**, 611 (2013).
[14] B. Schuler, W. Liu, A. Tkatchenko, N. Moll, G. Meyer, A. Mistry, D. Fox, and L. Gross, Phys. Rev. Lett. **111**, 106103 (2013).
[15] N. Moll, L. Gross, F. Mohn, A. Curioni, and G. Meyer, New Journal of Physics **12**, 125020 (2010).
[16] J. Welker, A. J. Weymouth, and F. J. Giessibl, ACS Nano **7**, 7377 (2013).
[17] L. Gross, F. Mohn, N. Moll, B. Schuler, A. Criado, E. Guitián, D. Peña, A. Gourdon, and G. Meyer, Science **337**, 1326 (2012).
[18] A. Schwarz, H. Hölscher, S. M. Langkat, and R. Wiesendanger, AIP Conf. Proc. **696**, 68 (2003).
[19] M. Ternes, C. P. Lutz, C. F. Hirjibehedin, F. J. Giessibl, and A. J. Heinrich, Science **319**, 1066 (2008).
[20] B. J. Albers, T. C. Schwendemann, M. Z. Baykara, N. Pilet, M. Liebmann, E. I. Altman, and U. D. Schwarz, Nature Nanotechnology **4**, 307 (2009).
[21] F. J. Giessibl, Appl. Phys. Lett. **76**, 1470 (2000).
[22] T. R. Albrecht, P. Grütter, D. Horne, and D. Rugar, J. Appl. Phys. **69**, 668 (1991).
[23] U. Dürig, H. R. Steinauer, and N. Blanc, J. Appl. Phys. **82**, 3641 (1997).
[24] An STM setpoint of $I = 1\,\mathrm{pA}$, $V = 0.4\,\mathrm{V}$ was used between imaging. After interrupting the feedback loop the tip was vertically displaced by $\Delta z_{\mathrm{Cu}} = 3.2\,\text{Å}$ and $\Delta z_{\mathrm{NaCl}} = -0.2\,\text{Å}$ to reach $z' = 0$ on copper and NaCl, respectively.
[25] R. Endres, C. Fong, L. Yang, G. Witte, and C. Wöll, Comp. Mat. Sci. **29**, 362 (2004).
[26] F. Giessibl, Phys. Rev. B **56**, 16010 (1997).
[27] F. J. Giessibl, Rev. Mod. Phys. **75**, 949 (2003).
[28] F. Mohn, L. Gross, N. Moll, and G. Meyer, Nature Nanotechnology **7**, 227 (2012).
[29] The position of local minima of $\Delta f(z')$ spectra for Pentacene on Cu(111) vary over the molecule as it is not adsorbed entirely flat[14].
[30] A. J. Weymouth, T. Hofmann, and F. J. Giessibl, Science (2014), 10.1126/science.1249502.